



Case Study

Aerodynamic characteristics of multiple airfoils in tandem using Ansys Fluent

Developed and curated by the Ansys Academic Development Team

Ravindra Arjun Shirsath

education@ansys.com

Summary

Investigating an external flow past any solid object has always been fascinating as well as challenging. The strong need for computational solutions arises as not everything can be measured/observed experimentally. Thus, Ansys Fluent is a popular commercial CFD software with vast capabilities starting from geometry preparation, meshing, solutions and post processing makes it easy to predict accurate flow physics under various circumstances including internal/external, steady/unsteady, uniform/non-uniform, compressible/incompressible, rotational/irrotational and laminar/turbulent flows.

In the present case study, steady state simulations are performed over a single NACA 0012 airfoil and are compared with the existing literature to show the accuracy of the software. The investigations are further extended to two airfoils operating in tandem with a specified separation between them. The results include the variation of aerodynamic characteristics, pressure and velocity distribution and flow visualization. The present study will serve as a starting point for mechanical, aerospace engineering students to better understand the fundamental concepts associated with external aerodynamics along with the visualization of attached and separated flows.

Table of Contents

1. Introduction.....	3
2. Problem Statement	3
3. Geometry and Mesh.....	4
4. Solution Methodology.....	4
5. Results and Discussion	4
5.1 Single airfoil – Aerodynamic characteristics	4
5.2 Tandem airfoils – Aerodynamic characteristics	5
5.3 Tandem airfoils – Velocity and Pressure distribution	6
5.4 Tandem airfoils – Effect of downwash	9
6. Further Steps	10
7. References	10

1. Introduction

The aerodynamic characteristics of various airfoils have been investigated for over a century with the intention of finding an optimum shape that can produce better lift and lesser drag resulting in better aerodynamic efficiency. The airfoils are classified based on many different parameters and camber is one of those parameters. Based on the camber, the airfoils are classified in two basic categories as positively cambered airfoils as shown in Fig. 1(a) and symmetric airfoils as shown in Fig. 1(b). Though the possibility of negatively cambered airfoils exists, it's just an inverted positively cambered airfoil whose application is rarely seen and hence not considered here explicitly.

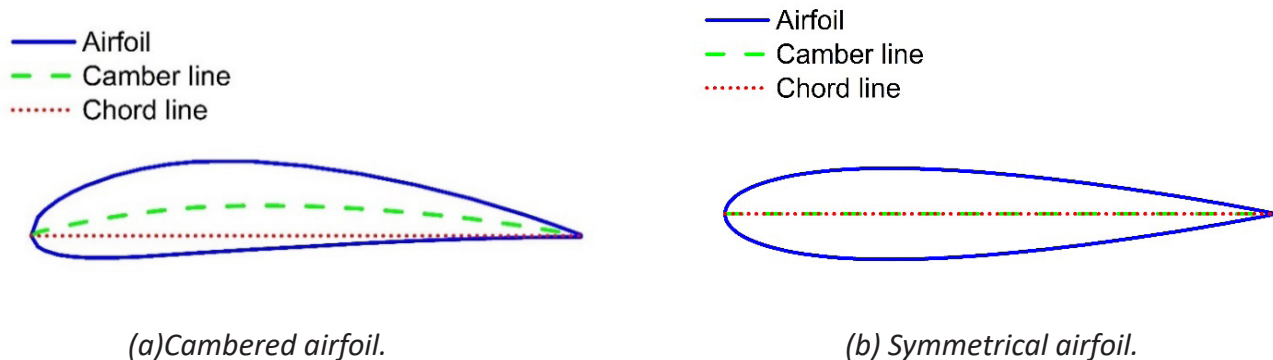


Figure 1. Classification of airfoils based on camber.

The important nomenclature associated with a general airfoil section is introduced here for clarity and most of these terminologies will be used in subsequent discussions.

- Chord line – It is defined as the straight line joining leading edge with trailing edge.
- Chord length (c) – The shortest distance between leading and trailing edges is called as chord length.
- Camber line – It is the line half-way between upper and lower surfaces of an airfoil.
- Leading edge – The foremost point of the chord-line is called leading edge.
- Trailing edge – The rearmost point of the chord-line is called trailing edge.
- Maximum thickness – It is the maximum distance between the upper and lower surface of an airfoil.
- Maximum camber – It is the maximum distance between the camber line and chord line.
- Angle of attack – It is an angle between the free stream velocity vector and the chord line of an airfoil.

2. Problem Statement

In the present work, first the traditional aerodynamic characteristics of a single airfoil are investigated and validated with the existing literature to understand the basics of flow phenomenon as it passes over an airfoil and get insights into the associated velocity and pressure distribution. Later the investigations are extended to two airfoils in tandem (one behind the other), over a wide range of angles of attack for a fixed separation between them as shown in Fig. 2. The angle of attack for both leading and trailing airfoils is varied simultaneously and is identical for every simulation. The attention is focused on the aerodynamic characteristics of both the airfoils, flow visualization, pressure distribution and variation in the downwash and associated changes in the aerodynamic performance of both the airfoils.



Figure 2. Airfoils in tandem.

3. Geometry and Mesh

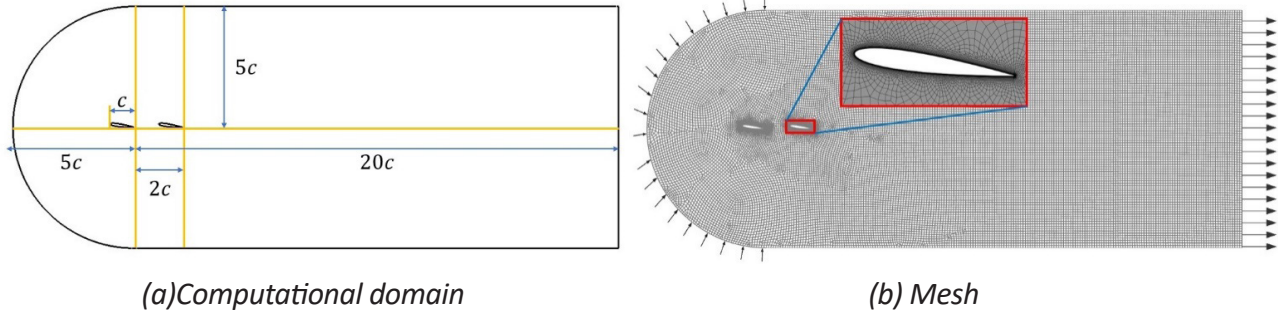


Figure 3. Details of the geometry, mesh and computational domain.

The airfoils considered for present study have NACA 0012 (symmetric) profile. The computational domain used is shown in Fig. 3(a) that extends $5c$ upstream as well as on top and bottom while $20c$ downstream as the downstream region is mostly influenced by the presence of the airfoils. The trailing edge of single/leading airfoil coincides with the origin while the trailing airfoil is located at a distance of x/c downstream. The mesh used for single airfoil has $\sim 40,000$ elements while that for the tandem airfoils has elements. Highly refined mesh is employed in the vicinity of the airfoils with layers of inflation and specified first layer height of 4.5×10^{-6} to ensure that near wall phenomenon is captured correctly and the specific requirements of the selected turbulence model in terms of y^+ are met. Though the mesh contains both quadrilateral and triangular elements, most of the domain predominantly consists of quadrilateral elements as seen from Fig. 3(b).

4. Solution Methodology

This section explains briefly the methodology adapted for steady-state CFD simulations using ANSYS Fluent. Numerical solver is set up with pressure-based type, absolute velocity formulation and pressure-velocity coupling is dealt with coupled algorithm. The working fluid is chosen to be an air with density $\rho = 1.225 \text{ kg/m}^3$ and dynamic viscosity, $\mu = 1.7894 \times 10^{-5} \text{ kg/m-s}$. Least square cell-based method is employed for estimating the gradients while second order upwind scheme is used for discretizing the equations. The velocity at inlet is specified to be in the streamwise direction corresponding to the Reynolds number $Re = 6 \times 10^6$ with the default turbulence properties, while outlet of the domain is imposed with the pressure outlet condition. Zero-gauge pressure is initialized throughout. The boundary at the airfoils is modeled to be solid wall and the same is imposed on the top and bottom of the domain. The selection of turbulence model is crucial, especially for the flows at higher angles of attack. When using $k-\omega$ (SST) model, our computational results are seen to agree fairly well with the experimental results as shown in Fig. 4, hence, $k-\omega$ (SST) is used throughout the analysis. The criterion for convergence is set to be 10^{-5} and additionally the force coefficients on the airfoil(s) are monitored individually ensuring that the simulations are run for the sufficient number of iterations.

5. Results and Discussion

5.1 Single airfoil – Aerodynamic characteristics

First the results are presented for single airfoil as seen from Fig. 4, the lift coefficient, C_L increases linearly with angle of attack, α up to approximately and then falls off drastically due to flow separation.

The results are compared with the existing literature to ensure that the properties and flow physics is captured correctly. The C_L predicted with the present study is seen to be in a fair agreement with those of Abbott *et. al.* and Gregory *et. al.*

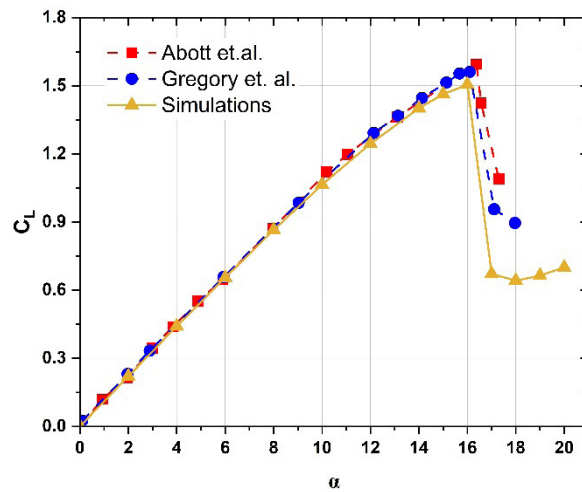
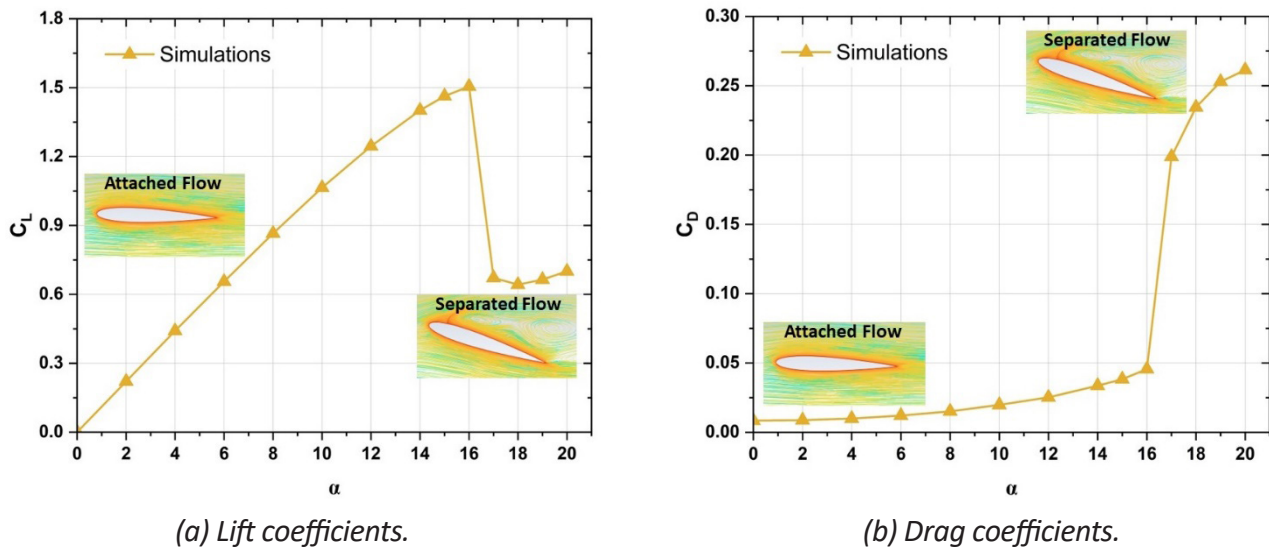


Figure 4. Lift coefficient of single airfoil.



(a) Lift coefficients.

(b) Drag coefficients.

Figure 5. Aerodynamic coefficients of single airfoil

The flow separation beyond 16° not only decreases the lift coefficient, C_L , drastically as seen from Fig. 5(a) but also increases the drag coefficient, C_D , by a considerable amount as shown in Fig. 5(b) thus it is generally advised to operate at a smaller angle of attack. The phenomenon of flow separation and associated loss of lift and rise of drag is known as stall and can be dangerous.

5.2 Tandem airfoils – Aerodynamic characteristics

Now the main objective of this study is to investigate what happens if there is a secondary lifting surface such as a trailing airfoil, how the overall aerodynamic characteristics of both the airfoils are influenced due to the presence of each other as well as due to the vortex-body interaction.

Thus, the results are presented in terms of lift and drag coefficients of both the leading and trailing airfoils over the range of angles of attack when the separation between them is $x/c=2$, *i.e.* the trailing

edge of trailing airfoil is two chord lengths behind that of the leading airfoil as shown in Fig. 2. It is interesting to observe that not only the performance of trailing airfoil is affected due to the presence of leading airfoil but also that of the leading airfoil is greatly influenced and that too favorably in terms of improved C_L and reduced C_D for smaller range of angles of attack *i.e.*, $\alpha < 12^\circ$ as seen from Fig 6(a) and (b). However, that of the trailing airfoil is affected adversely. An important observation from the aerodynamic characteristics is that the stalling angle is seen to reduce from 16° for the single airfoil to 12° for both leading and trailing airfoils when in tandem. Also, the leading airfoil is observed to be experiencing mild negative C_D for $0 < \alpha < 12^\circ$ which seems very promising while that drastically shoots up for . The performance of trailing airfoil however is seen to be affected mildly such that the loss of C_L and rise of C_D even in the post stall region is not very drastic.

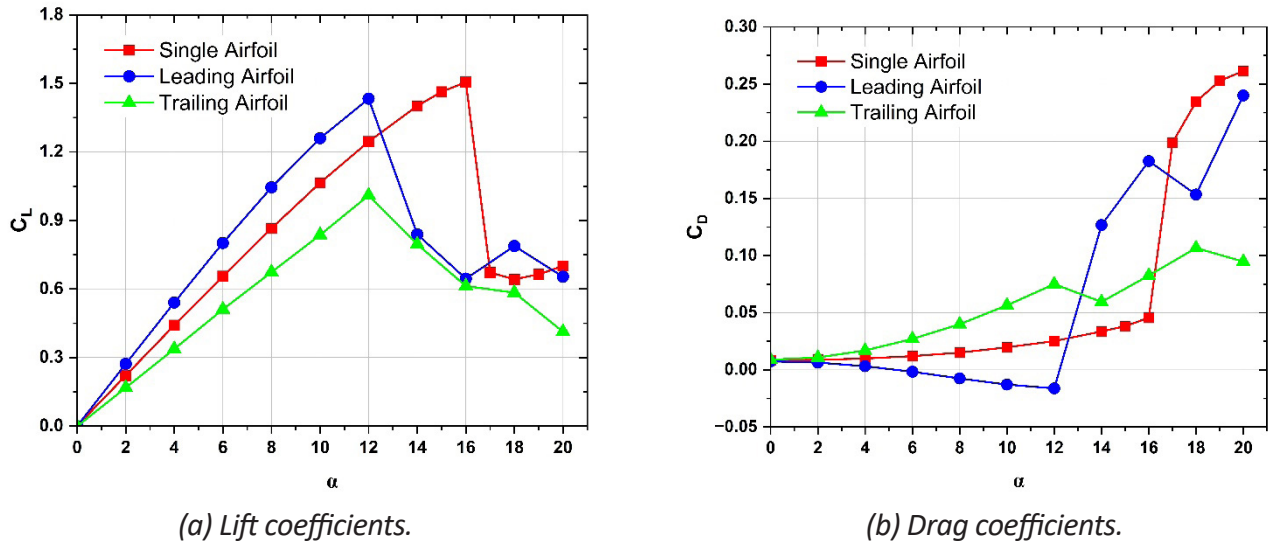
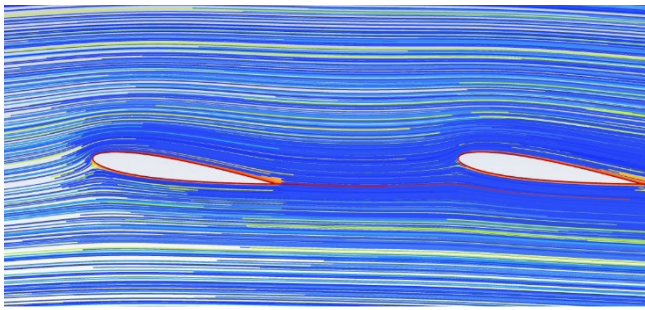


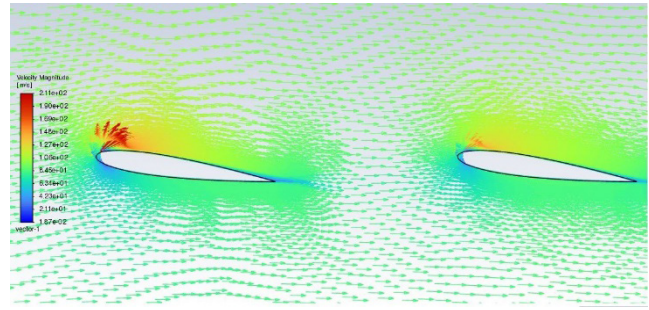
Figure 6. Aerodynamic coefficients of single and two airfoils in tandem, $x/c=2$

5.3 Tandem airfoils – Velocity and Pressure distribution

To get a better insight into what causes this varied performance of respective airfoils, the variation of downwash and pressure distribution over the airfoil is further investigated. The flow remains attached throughout on both the airfoils as visualized using the path lines at $\alpha=8^\circ$ as seen from Fig. 7(a) while corresponding velocity vector plot is shown in Fig. 7(b). Since no irregular changes are observed in the flow field the aerodynamic characteristics too vary smoothly however the reason for improved C_L and reduced C_D of the leading airfoil is not immediately clear and the inverse happening in case of trailing airfoil also remains unclear, thus there occurs a need to closely look into the velocity/pressure distribution and variation of y-component of velocity in particular as that has an important effect on the angle of attack and thus the aerodynamic characteristics.

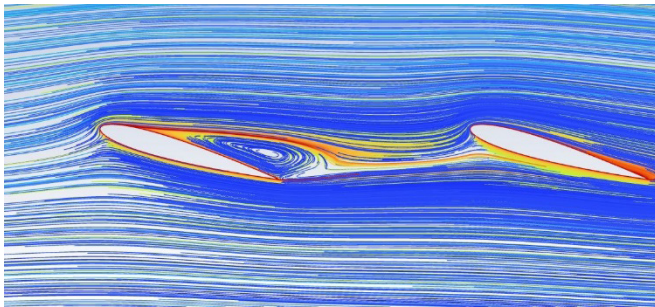


(a) Path lines.

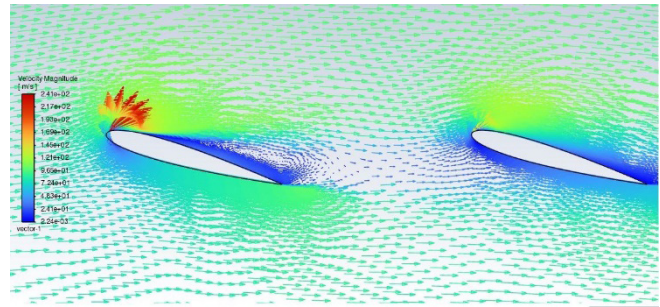


(b) Velocity vectors.

Figure 7. Flow visualization, $\alpha=8^\circ$



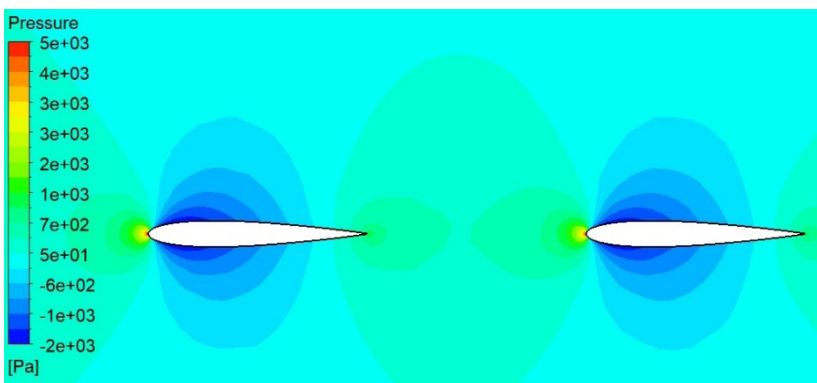
(a) Path lines.



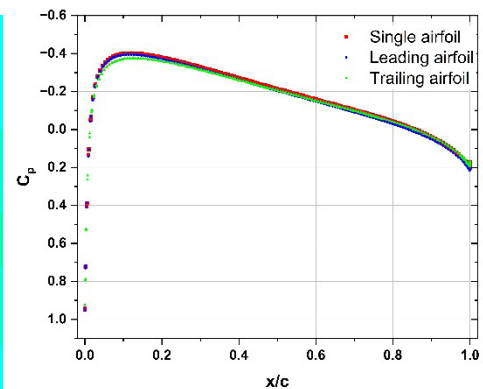
(b) Velocity vectors.

Figure 8. Flow visualization, $\alpha=16^\circ$

With increase in angle of attack, a clear flow separation is visible from path line plot as shown in Fig. 8(a) at $\alpha=16^\circ$ with associated velocity vector plots shown in Fig. 8(b). When this separated flow interacts with the trailing airfoil, it is evident that its aerodynamic characteristics are going to be affected to a larger extent and the same was visible in terms of C_l and C_d earlier in Fig. 6.



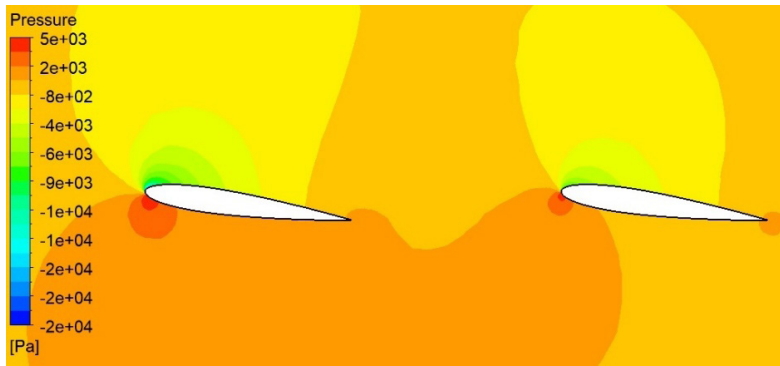
(a) Pressure contours.



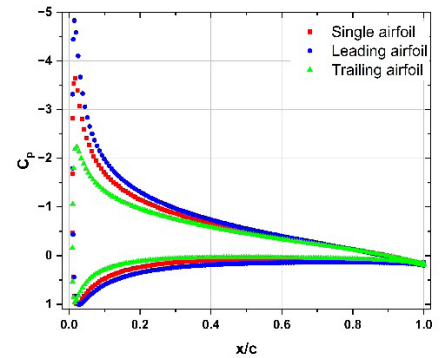
(b) plot

Figure 9. Pressure distribution, $\alpha=0^\circ$

The contours of pressure at $\alpha=0^\circ$ as shown in Fig. 9(a) clearly indicates that being a symmetric airfoil, the variation is identical on both the upper and lower surfaces and thus no lift force is experienced by either of the airfoils, the same is plotted in terms of a pressure coefficient, C_p over the airfoils in Fig. 9(b) which justifies the fact that at $\alpha=0^\circ$, nothing great happens in the flow field.



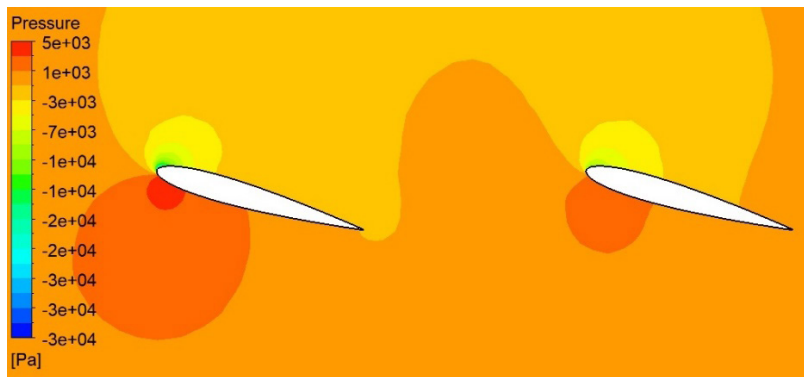
(a) Pressure contours.



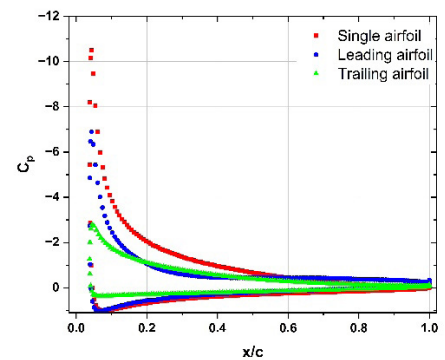
(b) C_p vs. x/c plot

Figure 10. Pressure distribution, $\alpha=8^\circ$

The area of C_p vs. x/c plot graph being a direct indicator of the lift clearly shows from Fig. 10(b) that at $\alpha=8^\circ$, the pressure distribution is no more identical and the leading airfoil has a greater C_L compared to the trailing airfoil which is primarily due to more region of reduced pressure on the upper surface as also is evident from the pressure contours shown in Fig. 10(a). Thus at this angle of attack, the leading airfoil experiences better C_L and trailing airfoil experiences lesser C_L compared to a single airfoil.



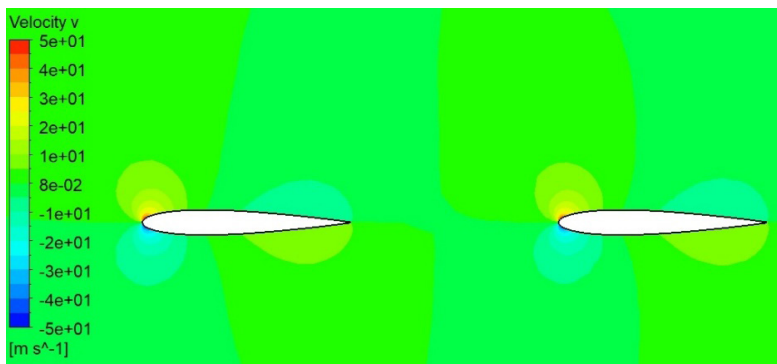
(a) Pressure contours.



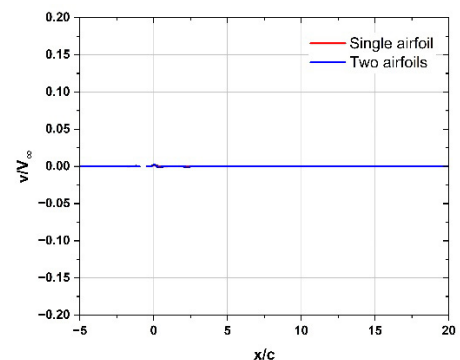
(b) C_p vs. x/c plot

Figure 11. Pressure distribution, $\alpha=16^\circ$

With further increase in angle of attack to $\alpha=16^\circ$, the pressure contours as shown in Fig. 11(a) are still different, however at this angle the C_p distribution of single airfoil has a maximum area as seen from Fig. 11(b) indicating the corresponding case now has a highest C_L while that of the leading and trailing airfoils is nearly identical.



(a) y -velocity contours.



(b) v/V_∞ vs. x/c plot

Figure 12. y -velocity distribution, $\alpha=0^\circ$

5.4 Tandem airfoils – Effect of downwash

The investigations are further extended to understand the variation of y-component of velocity as it directly influences the angle of attack. As seen from Fig. 12(a), at $\alpha=0^\circ$ there is not much variation in \mathbf{v} which justifies earlier observation that being a symmetric airfoil, at this angle of attack the $C_L=0$ and corresponding pressure distribution is identical between upper and lower surfaces. Corresponding non-dimensional component \mathbf{v}/V_∞ is plotted for the entire domain in Fig. 12 (b) that further justifies the observation as there is no variation in \mathbf{v}/V_∞ throughout the domain.

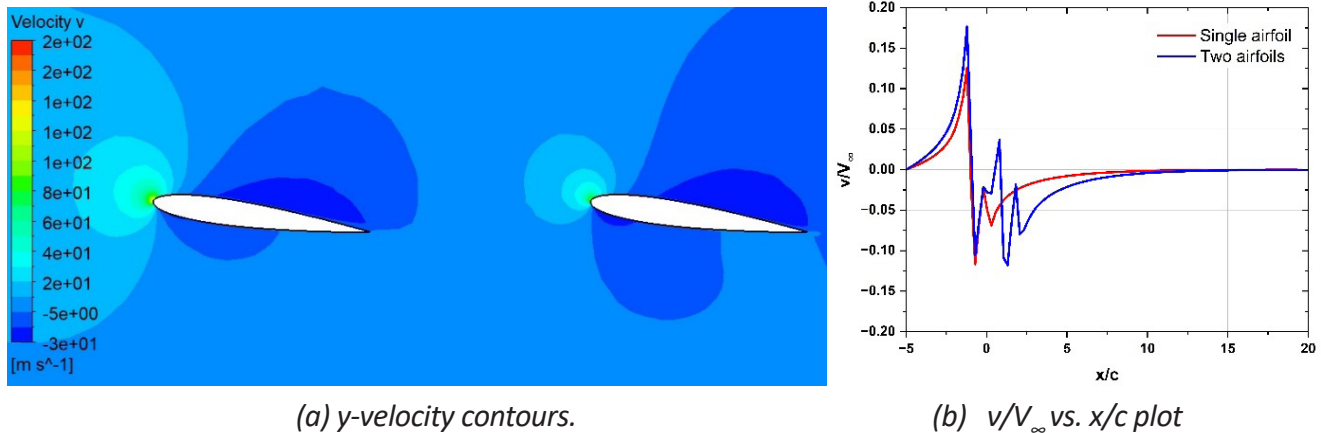


Figure 13. y-velocity distribution, $\alpha=8^\circ$

Interestingly, when the two airfoils are in tandem with $x/c=2$, at $\alpha=8^\circ$, there seems to be a considerable effect of as seen from y-velocity contours in Fig. 13(a) that there is an upward component of velocity near the leading edges of both the airfoils while it is marginally higher at the leading airfoil in tandem compared to single airfoil. The same is seen from Fig. 13(b), and it is this effect that causes relatively higher C_L for leading airfoil while the abrupt variation of \mathbf{v}/V_∞ over $0 < x/c < 5$ is responsible for the adversely affected aerodynamic performance of the trailing airfoil as compared to that of the single airfoil. The effect is seen to be diminishing further downstream as for $\mathbf{v}/V_\infty \rightarrow 0$ for $x/c > 10$.

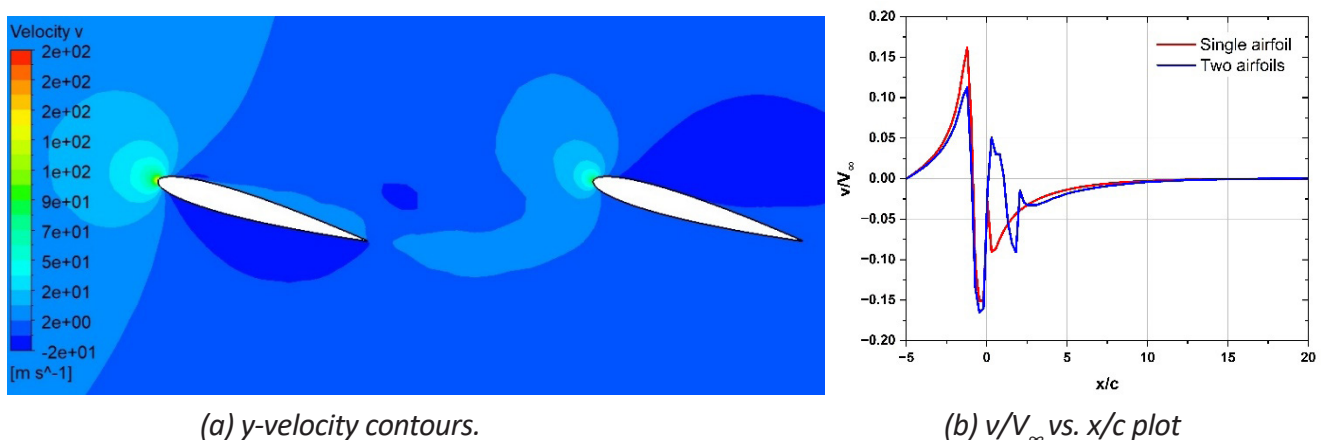


Figure 14. y-velocity distribution, $\alpha=16^\circ$

The increase in angle of attack to $\alpha=16^\circ$ is further seen to considerably affect the y-velocity contours as observed from Fig. 14(a), now the negative component of y-velocity is observed on lower surface of leading airfoil and upper surface of trailing airfoil, however the upwash in this case is observed to be relatively lesser compared to that of the single airfoil hence the C_L of leading airfoil in tandem is observed to be lesser compared to single airfoil. Also, the negative variation in \mathbf{v}/V_∞ is observed to be

of higher magnitude compared to the previous cases. Thus, overall, the airfoils in tandem are observed to be greatly influenced due to this irregularity of the flow pattern and thus resulting in lesser C_L and higher C_D at higher angles of attack when compared to the single airfoil, however at lower angles of attack, a considerable improvement in the aerodynamic performance of leading airfoil is observed.

6. Further Steps

In the present case study, the aerodynamic characteristics of a single airfoil and two airfoils in tandem with the specified separation between them are investigated using Ansys Fluent. The results obtained for a single airfoil are seen to fairly match with the experimental data available in the literature. The investigation clearly shows that complex flow phenomenon can be observed around two airfoils in tandem, and how these can be investigated using advanced CFD software such as Ansys Fluent to predict the aerodynamic characteristics of both the airfoils along with the flow visualization using path lines, pressure and velocity contours and to quantify the same in terms of the variation of y-component of velocity.

The investigations show preliminary analysis and the same can be extended to further investigate the effect of separation between the airfoils, effect of thickness and camber of the airfoils, effect of fixing an angle of attack of one of the airfoil and then varying the other, changing the vertical location of the trailing airfoil as well to find the optimum position for best aerodynamic performance etc.

7. References

1. 2D NACA 0012 Airfoil Validation Case, NASA Langley Research Center, Turbulence Modeling Resources, 2DN00.
2. Charles L. Landson, Effects of Independent Variation of Mach and Reynolds Numbers on the Low-Speed Aerodynamic Characteristics of the NACA 0012 Airfoil Section, NASA Technical Memorandum 4074, 1988.
3. Gregory N. and O'Reilly C. L., Low-Speed Aerodynamic Characteristics of NACA 0012 Airfoil Section, including the Effect of Upper Surface Roughness Simulating Hoar Frost, Ministry of Defence, Aeronautical Research Council, Reports and Memoranda No. 3726, 1970.

© 2024 ANSYS, Inc. All rights reserved.

Use and Reproduction

The content used in this resource may only be used or reproduced for teaching purposes; and any commercial use is strictly prohibited.

Document Information

This case study is part of a set of teaching resources to help introduce students to topics related to fluids.

Ansys Education Resources

To access more undergraduate education resources, including lecture presentations with notes, exercises with worked solutions, microprojects, real life examples and more, visit www.ansys.com/education-resources.

Feedback

If you notice any errors in this resource or need to get in contact with the authors, please email us at education@ansys.com.

ANSYS, Inc.
Southpointe
2600 Ansys Drive
Canonsburg, PA 15317
U.S.A.
724.746.3304
ansysinfo@ansys.com

If you've ever seen a rocket launch, flown on an airplane, driven a car, used a computer, touched a mobile device, crossed a bridge or put on wearable technology, chances are you've used a product where Ansys software played a critical role in its creation. Ansys is the global leader in engineering simulation. We help the world's most innovative companies deliver radically better products to their customers. By offering the best and broadest portfolio of engineering simulation software, we help them solve the most complex design challenges and engineer products limited only by imagination.

visit www.ansys.com for more information

Any and all ANSYS, Inc. brand, product, service and feature names, logos and slogans are registered trademarks or trademarks of ANSYS, Inc. or its subsidiaries in the United States or other countries. All other brand, product, service and feature names or trademarks are the property of their respective owners.

© 2024 ANSYS, Inc. All Rights Reserved.